NLO CORRECTIONS TO $h \to WW/ZZ \to 4$ FERMIONS IN A SINGLET EXTENSION OF THE STANDARD MODEL*

Michele Boggia, Stefan Dittmaier

Albert-Ludwigs-Universität Freiburg, Physikalisches Institut
79104 Freiburg, Germany

(Received January 22, 2018)

At the LHC, the properties of the Higgs boson are investigated to search for traces of physics beyond the Standard Model (SM), with the aim of making discoveries via precision measurements. To this end, theoretical predictions at the highest possible accuracy are required, both within the SM and its extensions. Singlet extensions (SESMs) supplement the SM by a scalar $\mathrm{SU}(2)_W$ gauge singlet, replacing the single Higgs boson of the SM by two CP-even Higgs bosons. The SM coupling strength is shared by the two Higgs bosons, *i.e.* the Higgs bosons couple with the SM strength weighted by the sine or cosine of a mixing angle. The mass of the additional Higgs boson, the mixing angle, and possibly one or more couplings of the scalar self-interactions parametrize the extended sector. The program Prophecy4f, which calculates decay observables for $h \to WW/ZZ \to 4$ fermions with EW and QCD corrections in the SM, has been upgraded to an SESM and used to quantify the deviations induced by the extension. We summarize the basic features of the considered extension and the most important numerical results on the predictions for the Higgs decays to four fermions.

DOI:10.5506/APhysPolBSupp.11.285

1. Introduction

The current SM of particle physics cannot be the ultimate theory to describe nature, since some observed phenomena, such as the presence of dark matter, the evidence for massive neutrinos, and the baryon asymmetry of the universe, are not explained by the theory. However, the data collected at the LHC from the experiments ATLAS and CMS show a good agreement with the SM predictions. The resonance discovered in 2012 [1, 2] resembles

* Presented at the Final HiggsTools Meeting, Durham, UK, September 11–15, 2017.

the SM Higgs boson, and no significant deviations are seen at the scales covered by the LHC. Nevertheless, as the experimental accuracy improves collecting more data, there is still room to observe small deviations. If this is the case, in order to characterize the origin of the deviations, precise theoretical predictions will be required not only for the SM, but also for beyond the SM (BSM) theories. In our research, we considered an SESM [3–5], consisting in the SM supplemented by a real scalar gauge singlet, and we implemented the decay process of the light Higgs into four fermions in the Monte Carlo program Prophecy4f [6,7], assuming that the light scalar of the theory is the resonance observed at 125 GeV [1,2]. The program can be used to compute the decay widths for all the possible four-fermion final states. Moreover, for each four-lepton final state (and semi-leptonic final states to some extent), it allows to generate mass and angular distributions and unweighted events.

In Section 2, we introduce the basic features of the SESM, in Section 3, we give a short description of the decay process $h \to WW/ZZ \to 4$ fermions, in Section 4, we outline the implementation of the calculation in Prophecy4f, and we present a selection of our results in Section 5. A summary of the work is reported in Section 6.

2. Singlet extension of the Standard Model

2.1. Model description

The Higgs Lagrangian of the SESM is given by the SM Higgs Lagrangian for the complex doublet Φ, supplemented by a kinetic term for the real singlet field σ, and all the possible multi-scalar interactions compatible with gauge-invariance and renormalizability. We impose an extra $\mathbb{Z}_2$ symmetry, dropping terms containing an odd number of singlet fields, obtaining

$$\mathcal{L}_{\text{Higgs}}^{\text{SESM}} = (D_\mu \Phi)^\dagger (D^\mu \Phi) + \frac{1}{2}(\partial_\mu \sigma)(\partial^\mu \sigma) - V(\Phi, \sigma)\,,$$
$$V(\Phi, \sigma) = -\mu_2^2 \Phi^\dagger \Phi + \frac{\lambda_2}{4}\left(\Phi^\dagger \Phi\right)^2 + \lambda_{12}\sigma^2 \Phi^\dagger \Phi - \mu_1^2 \sigma^2 + \lambda_1 \sigma^4\,.$$

The complete Lagrangian of the model can be obtained replacing, in the full SM Lagrangian, $\mathcal{L}_{\text{Higgs}}$ by the expression given above. The $\mathbb{Z}_2$ symmetry can be interpreted as the real counterpart of a hidden U(1) symmetry inducing interactions in a dark sector (as discussed, *e.g.*, in Ref. [8]). We focus on the case in which the symmetry is broken by the non-vanishing vacuum expectation values v_2, for the doublet, and v_1, for the singlet. The scalar fields are parametrized by

$$\Phi = \begin{pmatrix} \phi^+ \\ \frac{1}{\sqrt{2}}\left[v_2 + h_2 + \mathrm{i}\phi^0\right] \end{pmatrix}, \qquad \sigma = v_1 + h_1\,.$$

After symmetry breaking, the Higgs potential contains a non-diagonal mass matrix, which can be diagonalized applying a rotation on the fields h_2 and h_1 about an angle α

$$\begin{pmatrix} h \\ H \end{pmatrix} = \begin{pmatrix} c_\alpha & -s_\alpha \\ s_\alpha & c_\alpha \end{pmatrix} \begin{pmatrix} h_2 \\ h_1 \end{pmatrix} ,$$

where $c_\alpha \equiv \cos\alpha$ and $s_\alpha \equiv \sin\alpha$, and requiring that the fields h and H do not mix at leading order (LO). In this way, it is possible to trade the parameters $\mu_2, \mu_1, \lambda_2, \lambda_1$ for the boson masses M_h, M_H and the tadpole constants t_h, t_H (which vanish at tree level). We enforce the hierarchy $M_h < M_H$ and assign the mass of the observed Higgs boson to the field h, so that only three parameters (M_H, λ_{12}, and α) can be fixed freely. The total Lagrangian of the theory provides two copies of the SM Higgs couplings to non-scalar particles, one rescaled by a factor c_α, for the light field h, and one rescaled by s_α, for H. Moreover, new multi-scalar interactions arise from the Higgs potential, and the SM Higgs self-interactions are non-trivially modified. For these reasons, despite the simplicity of the model, the SESM offers an interesting phenomenology.

2.2. Renormalization

To perform next-to-leading order (NLO) computations within the SESM, we renormalize the theory introducing multiplicative renormalization constants for all the input parameters, as well as for the fields. To fix the renormalization constants, we adopt two renormalization schemes. In both schemes, we apply on-shell (OS) renormalization conditions as far as possible (see, *e.g.*, Ref. [9]), using $\overline{\text{MS}}$ conditions for the BSM parameters α and λ_{12}. $\overline{\text{MS}}$ renormalization conditions are used, because there is no evidence for a singlet-like scalar, and it is not clear how to relate the renormalized parameters α and λ_{12} to physical quantities. The two renormalization schemes differ only in the treatment of the tadpoles. In the first scheme, the renormalized tadpole constants are set to zero (as usual within OS renormalization [9]), so that tadpole diagrams can be discarded when performing loop calculations. The drawback of this choice is that the gauge-dependent tadpoles enter relations among bare parameters, and could lead to gauge-dependent results. In the second scheme, we set to zero the bare tadpole constants, following an approach equivalent to the treatment described in Refs. [10–13]. In the following, we will refer to the two schemes as the $\overline{\text{MS}}$ and Fleischer–Jegerlehner (FJ) schemes.

3. The decays $h \to WW/ZZ \to 4$ fermions

The decays into four fermions via two vector bosons played a central role in the discovery of the Higgs boson and are promising channels for precise Higgs measurements. The decays were implemented in the Monte Carlo generator Prophecy4f for the SM [6, 7] and for the two-Higgs-doublet model (THDM) [14, 15], including NLO EW and QCD corrections, and we extended the program with the SESM. The generator can be used to compute the partial widths of the decays into four light fermions, and to produce differential distributions. The final-state fermions are taken in the massless limit, but the physical masses are retained in closed fermion loops. Since the mass of the SM-like Higgs boson is below the threshold for the production of a W- or Z-boson pair, the intermediate W- and Z-boson resonances are treated in the complex-mass scheme [16, 17]. The phase-space integration is performed numerically by the multi-channel Monte Carlo integrator implemented in the original Prophecy4f version.

Exemplary diagrams contributing to the decays are reported in Fig. 1. The tree diagram on the left is the only diagram structure at tree level, and the corresponding matrix element can be obtained rescaling the SM expression, since the only modification is the additional factor c_α in the hVV coupling. At NLO, more contributions are taken into account, where the heavy scalar H can appear as a virtual particle. In the computation, we include all the EW and QCD loops, and we show in the figure only one exemplary diagram. The third diagram reported in Fig. 1 is an example of a counterterm contribution coming from the renormalization procedure. Similar diagrams exist, with counterterm insertions on the vector propagators and on the Vff vertices and are not shown here. The last diagram of Fig. 1 corresponds to real photon emission which, together with gluon emission, has been consistently taken into account in order to have infrared (IR) finite results. In this regard, we treat the cancellation of IR contributions using slicing and dipole-subtraction methods [18–20]. Similarly to the LO diagram, also the real-emission diagrams can be obtained by rescaling the corresponding SM expressions by a factor c_α.

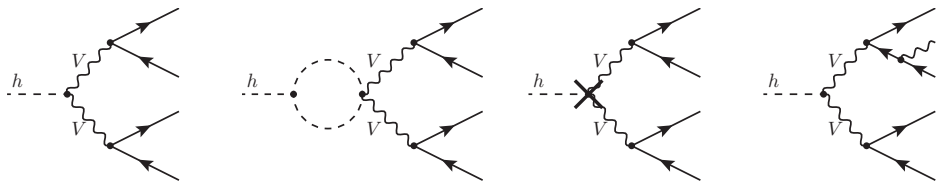

Fig. 1. Exemplary diagrams contributing to the decays $h \to WW/ZZ \to 4f$. From left to right: LO diagram, example of an EW loop with scalar exchange, counterterm, and real emission diagram.

4. Automation

We used the MATHEMATICA package FEYNRULES [21, 22] to produce, starting from the Lagrangian of the SESM, a model file that allows, with the packages FEYNARTS and FORMCALC [23, 24], to generate and simplify NLO (EW and QCD) matrix elements, including all the counterterm contributions. We intensively tested the model file checking UV-finiteness for many processes (both analytically and numerically) giving special attention to the multi-scalar vertex functions, which involve the renormalization constants of the mixing angle α and the coupling λ_{12}. Then, we adapted the model file to produce matrix elements suitable for our analysis of the decay processes $h \to WW/ZZ \to 4$ fermions, introducing complex vector-boson masses and massless final-state fermions. The obtained model file has been used to compute the squared matrix elements for the process and to produce, using FORMCALC, the FORTRAN routines for the numerical evaluation in PROPHECY4F. All ingredients of the computation were checked by an independent calculation using a user-defined FEYNARTS model file, in-house MATHEMATICA routines for the algebraic reduction, and the library COLLIER [25] for the evaluation of the loop integrals. The obtained program can be used to compute the decay widths for the considered processes, as well as differential distributions for all the possible four-fermion final states. For leptonic final states, the generation of unweighted events is supported.

5. Numerical results

For the numerical analysis, we consider four of the benchmark scenarios proposed in Refs. [26, 27], converting the input parameters to our conventions. In the following, we present a selection of the most relevant results obtained in the scenario BHM200, defined by the input values

$$\text{BHM200:} \quad M_H = 200 \text{ GeV}\,, \qquad s_\alpha = 0.29\,, \qquad \lambda_{12} = 0.07\,.$$

Since we consider two renormalization schemes, we consistently convert the input parameters between the two schemes. In our case, the mixing angle is the only parameter for which such a conversion is required, and we numerically solve the equation

$$s_{\alpha,0} = s_\alpha^{\overline{\text{MS}}} + \delta s_\alpha^{\overline{\text{MS}}}\left(s_\alpha^{\overline{\text{MS}}}\right) = s_\alpha^{\text{FJ}} + \delta s_\alpha^{\text{FJ}}\left(s_\alpha^{\text{FJ}}\right)\,,$$

i.e. the renormalized parameters $s_\alpha^{\overline{\text{MS}}/\text{FJ}}$ are translated into each other by matching them to the bare parameter $s_{\alpha,0}$, which is independent of the renormalization scheme. The left panel of Fig. 2 shows the result for $s_\alpha^{\overline{\text{MS}}}(s_\alpha^{\text{FJ}})$,

where large conversion effects are evident for small values of the mixing angle. These effects are loop induced (in principle small), but approaching small α values, the perturbativity of the Lagrangian couplings breaks down, leading to large contributions to the conversion. For this reason, the area around $s_\alpha = 0$ is shaded in the plot. Another important step towards the computation of NLO observables is the solution of the renormalization group equations (RGEs) for the parameters defined by $\overline{\text{MS}}$ conditions which are, in our case, the mixing angle α and λ_{12}. Indeed, due to the renormalization procedure, the NLO predictions for observables depend on the renormalization scale μ_r. Thus, it is important to analyze and minimize the dependence of the final results on this unphysical scale. The right panel of Fig. 2 shows the variation of the sine of the mixing angle for a scale variation in the range $\mu_\text{r} = 40$–375 GeV, for both renormalization schemes. For consistency, we account also for the running of the coupling λ_{12}, which enters only the loop corrections and has a smaller impact on the scale dependence of the final results. Since this is a sub-leading effect, we do not show here the dependence of λ_{12} on the renormalization scale.

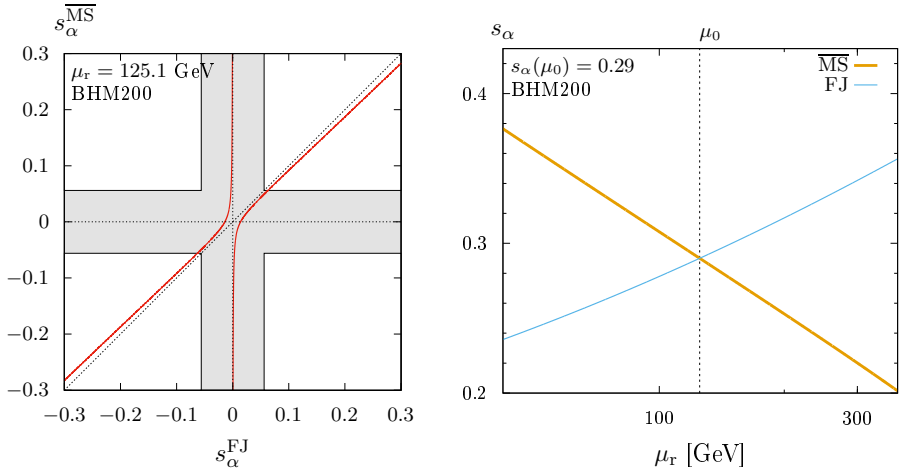

Fig. 2. On the left, scheme conversion for s_α. On the right, numerical solution of the RGEs for s_α in the $\overline{\text{MS}}$ and FJ renormalization schemes, for input values fixed at the initial scale $\mu_0 = M_h$.

In order to choose a reasonable renormalization scale, we study the scale dependence of the total decay width $\Gamma^{h\to 4f}$. For this purpose, we evolve the input values for α and λ_{12} from the input scale $\mu_0 = M_h$ to the scale μ_r and compute both the LO and the NLO widths at different renormalization scales in the range of $\mu_\text{r} = 40$–375 GeV. In the left panel of Fig. 3, we show the results obtained fixing the input parameters in the FJ scheme, and computing the decay widths both in the $\overline{\text{MS}}$ and the FJ renormalization

schemes. Dashed lines correspond to LO results, solid lines are obtained including NLO EW corrections. To obtain the results in the $\overline{\text{MS}}$ scheme, we first convert the input parameters at the initial scale μ_0 and then compute the decay width in the $\overline{\text{MS}}$ scheme. The improvement driven by the inclusion of the NLO corrections is remarkable: The scale dependence of the decay width is reduced in both renormalization schemes, and the scheme dependence (difference of predictions in the two schemes) is reduced as well. Moreover, we observe that the scale choice $\mu_0 = M_h$ represents a reasonable choice for our calculations. The alternative scale choice given by the arithmetic mean of the Higgs masses proposed in Refs. [14, 15] for the THDM does not fit the SESM case. Indeed, for scenarios with higher M_H values, the alternative scale $\mu_r = (M_h + M_H)/2$, is always far away from the region where the scale dependence is minimal.

The main goal of our work is to inspect the deviations from the SM induced by the inclusion of the singlet. To this end, we study how the total decay width $\Gamma^{h\to 4f}$ depends on the BSM parameters. Among these parameters, the mixing angle plays the central role, since its value affects already the LO result, while the heavy Higgs mass M_H and the coupling λ_{12} enter only in the NLO decay amplitude. For this reason, we compute the total decay width scanning over different values for the mixing angle in the range of $|s_\alpha| < 0.3$, keeping M_H and λ_{12} fixed. In the right panel of Fig. 3, we report the results, together with the SM results, which are represented by the horizontal lines. As before, we present the results in both renormalization schemes. Dashed lines correspond to LO results, while solid lines include NLO EW and QCD contributions. The input scheme used

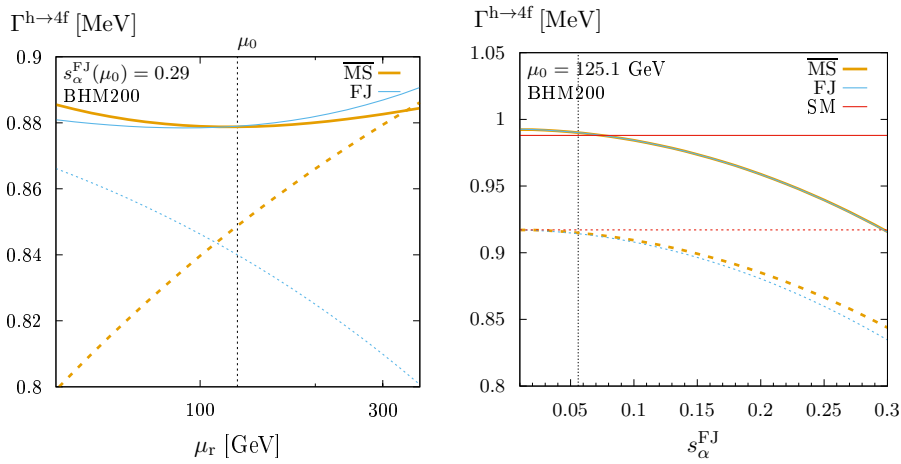

Fig. 3. Scale dependence of the width $\Gamma^{h\to 4f}$ in the scenario BHM200 (left) and comparison with the SM value, as a function of s_α, with M_H and λ_{12} fixed according to the scenario BHM200 (right).

is FJ, and the input values used for M_H and λ_{12} are the values corresponding to the scenario BHM200. For the computation, we use the renormalization scale $\mu_0 = M_h$. The vertical dashed line marks the small-s_α region where perturbativity problems can arise. Indeed, in scenarios with higher values for the heavy mass M_H, we observe large conversion effects for small s_α values. The LO results for the SESM, compared to the SM, display the expected c_α^2 behaviour. The inclusion of NLO corrections reduces the scheme dependence (the NLO results for the two schemes overlap in the plot) and compensates, for small α values, the c_α^2 suppression. In general, we observe that the relative deviations from the SM are always smaller than 10% for the considered benchmark points.

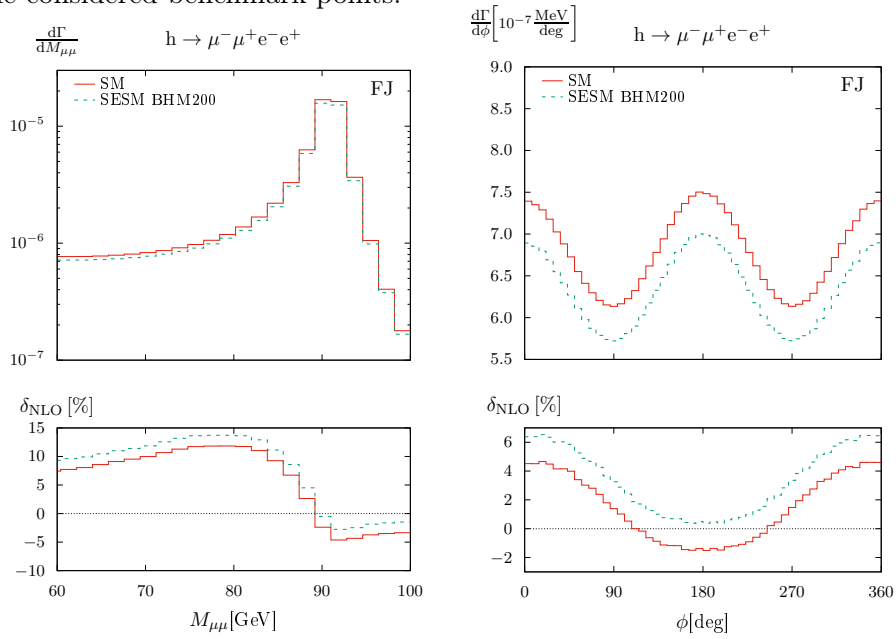

Fig. 4. Distributions for the muon-pair invariant mass (left) and for the angle between the decay planes of the two Z bosons (right), for the decay $h \to \mu^-\mu^+e^-e^+$ in the SM and in the scenario BHM200. The lower panels report the relative NLO corrections.

In general, footprints of BSM physics may be found looking in the shape of differential distributions, even if the integrated results do not deviate from the SM. We use our implementation to generate differential distributions for leptonic and semi-leptonic final states and report in Fig. 4 two examples, which show a common feature that we observed in all the distributions. Indeed, the relative NLO corrections δ_{NLO} for the SESM, reported in the lower panels, are equal to the SM case up to a constant offset, which is the same for all the distributions.

6. Conclusions

Extensions obtained by adding an extra singlet scalar to the SM offer an interesting phenomenology and are considered in the current experimental analysis as a possible candidate for the next SM. Considering an SESM with a $\mathbb{Z}_2$-symmetric scalar potential and EWSB both for the SM-like doublet and the singlet, we renormalized the theory using two schemes. The first scheme introduces gauge-dependent tadpoles in the relations among bare parameters, but can be used provided that subsequent calculations are performed using the same gauge. Using the second renormalization scheme, gauge-dependent terms cancel in the relations between the parameters, but explicit tadpoles must be taken into account when computing loop amplitudes. We studied the conversion between the two schemes observing sizable effects and solved the RGEs for the $\overline{\text{MS}}$ parameters. Making use of the MATHEMATICA packages FEYNRULES, FEYNARTS, and FORMCALC, we upgraded the Monte Carlo program PROPHECY4F, in order to calculate decay observables for $h \to WW/ZZ \to 4$ fermions with EW and QCD corrections in the SESM. With the program, we considered four benchmark scenarios proposed in the literature and computed the decay width for the inclusive decay $h \to 4$ fermions. We studied how the result depends on the renormalization scale and observe how the inclusion of NLO order corrections mitigate the scale and the scheme dependences, indicating proper convergence of the perturbative series in the considered scenarios. Comparing the decay width with the SM case, we find relative deviations below 10%. Finally, we generated kinematical distributions for the leptonic and semi-leptonic final states and observe that no additional distortions on top of the SM shape are induced. For a detailed description of the calculation and more results, see Ref. [28].

We thank L. Altenkamp for discussions and support. We thank the German Research Foundation (DFG) and Research Training Group GRK 2044 for the funding and the support and acknowledge support by the state of Baden-Württemberg through bwHPC and the DFG through grant No. INST 39/963-1 FUGG. We acknowledge the Research Executive Agency (REA) of the European Union for funding this work through the Grant Agreement PITN-GA-2012-316704 ("HiggsTools").

REFERENCES

[1] G. Aad *et al.* [ATLAS Collaboration], *Phys. Lett. B* **716**, 1 (2012) [arXiv:1207.7214 [hep-ex]].
[2] S. Chatrchyan *et al.* [CMS Collaboration], *Phys. Lett. B* **716**, 30 (2012) [arXiv:1207.7235 [hep-ex]].
[3] V. Silveira, A. Zee, *Phys. Lett. B* **161**, 136 (1985).

[4] M.J.G. Veltman, F.J. Yndurain, *Nucl. Phys. B* **325**, 1 (1989).
[5] J. McDonald, *Phys. Rev. D* **50**, 3637 (1994) [arXiv:hep-ph/0702143].
[6] A. Bredenstein, A. Denner, S. Dittmaier, M.M. Weber, *J. High Energy Phys.* **0702**, 080 (2007) [arXiv:hep-ph/0611234].
[7] A. Bredenstein, A. Denner, S. Dittmaier, M.M. Weber, *Phys. Rev. D* **74**, 013004 (2006) [arXiv:hep-ph/0604011].
[8] B. Patt, F. Wilczek, arXiv:hep-ph/0605188.
[9] A. Denner, *Fortsch. Phys.* **41**, 307 (1993) [arXiv:0709.1075 [hep-ph]].
[10] J. Fleischer, F. Jegerlehner, *Phys. Rev. D* **23**, 2001 (1981).
[11] S. Actis, A. Ferroglia, M. Passera, G. Passarino, *Nucl. Phys. B* **777**, 1 (2007) [arXiv:hep-ph/0612122].
[12] M. Krause *et al.*, *J. High Energy Phys.* **1609**, 143 (2016) [arXiv:1605.04853 [hep-ph]].
[13] A. Denner, L. Jenniches, J.N. Lang, C. Sturm, *J. High Energy Phys.* **1609**, 115 (2016) [arXiv:1607.07352 [hep-ph]].
[14] L. Altenkamp, S. Dittmaier, H. Rzehak, *J. High Energy Phys.* **1709**, 134 (2017) [arXiv:1704.02645 [hep-ph]].
[15] L. Altenkamp, S. Dittmaier, H. Rzehak, *J. High Energy Phys.* **1803**, 110 (2018) [arXiv:1710.07598 [hep-ph]].
[16] A. Denner, S. Dittmaier, M. Roth, D. Wackeroth, *Nucl. Phys. B* **560**, 33 (1999) [arXiv:hep-ph/9904472].
[17] A. Denner, S. Dittmaier, M. Roth, L.H. Wieders, *Nucl. Phys. B* **724**, 247 (2005) [*Erratum ibid.* **854**, 504 (2012)] [arXiv:hep-ph/0505042].
[18] S. Catani, M.H. Seymour, *Nucl. Phys. B* **485**, 291 (1997) [*Erratum ibid.* **510**, 503 (1998)] [arXiv:hep-ph/9605323].
[19] S. Dittmaier, *Nucl. Phys. B* **565**, 69 (2000) [arXiv:hep-ph/9904440].
[20] S. Dittmaier, A. Kabelschacht, T. Kasprzik, *Nucl. Phys. B* **800**, 146 (2008) [arXiv:0802.1405 [hep-ph]].
[21] N.D. Christensen, C. Duhr, *Comput. Phys. Commun.* **180**, 1614 (2009) [arXiv:0806.4194 [hep-ph]].
[22] A. Alloul *et al.*, *Comput. Phys. Commun.* **185**, 2250 (2014) [arXiv:1310.1921 [hep-ph]].
[23] T. Hahn, *Comput. Phys. Commun.* **140**, 418 (2001) [arXiv:hep-ph/0012260].
[24] T. Hahn, M. Pérez-Victoria, *Comput. Phys. Commun.* **118**, 153 (1999) [arXiv:hep-ph/9807565].
[25] A. Denner, S. Dittmaier, L. Hofer, *Comput. Phys. Commun.* **212**, 220 (2017) [arXiv:1604.06792 [hep-ph]].
[26] D. de Florian *et al.* [LHC Higgs Cross Section Working Group], CERN Yellow Reports: Monographs, DOI:10.23731/CYRM-2017-002 [arXiv:1610.07922 [hep-ph]].
[27] T. Robens, T. Stefaniak, *Eur. Phys. J. C* **76**, 268 (2016) [arXiv:1601.07880 [hep-ph]].
[28] L. Altenkamp, M. Boggia, S. Dittmaier, arXiv:1801.07291 [hep-ph], to appear in *J. High Energy Phys.*